All Optical Stabilization of a Monolithic Quantum Dot Based CPM Laser Via Four-Wave Mixing

Abhijeet Ardey, Edris Sarailou, *Student Member, IEEE*, and Peter J. Delfyett, *Fellow, IEEE*

***Abstract*— We investigate and confirm a four-wave mixing (FWM) process as the primary mechanism responsible for locking and stabilization of a previously reported novel quantum dot based monolithically coupled colliding pulse mode-locked (CPM) laser. In the previous letter, a high-Q passively mode-locked ring laser is used to injection lock an orthogonally coupled passively mode-locked CPM slave laser via FWM in the common saturable absorber. In this letter, we setup an experiment to verify the FWM process, whereby the external ring laser is operated unidirectionally while simultaneously analyzing the amplified spontaneous emission from the other facet of the ring laser. The emission is found to contain CPM light only in the presence of injection locking proving the FWM process. Other linear scattering effects are also investigated and shown to be negligible in the orthogonal waveguide configuration.**

***Index Terms*— Four-wave mixing, injection locking, mode-locked laser, quantum dot, timing jitter.**

I. Introduction

MONOLITHIC colliding pulse mode-locked (CPM) diode lasers provide compact and mechanically stable sources of ultrashort optical pulses and are promising devices for future large capacity optical communication networks. These include high-bit-rate optical time-division multiplexing (OTDM) systems and microwave/millimeter-wave photonic systems. Passively mode-locked CPM lasers using an intracavity saturable absorber (SA) provide nearly transform limited ultrafast optical pulse train without the need for high speed electronics. These lasers have been demonstrated to produce pico- to sub-picosecond pulses at repetition frequencies from 16 to 480 GHz [1], [2]. The performance is further expected to improve by employing quantum dot (QD) material as the active medium which has inherent properties such as low threshold current, fast carrier dynamics and modified density of states function [3]–[5]. With lower associated spontaneous emission noise as compared to quantum well (QW) devices, the linewidths are generally narrower in passive QD lasers [6]. However, the lack of a stable frequency reference source still leads to a considerable timing jitter in these lasers resulting in broad comb linewidths [7], which precludes many applications in the field of coherent communication and signal processing where a much narrower frequency line set is needed.

Recently, we proposed and demonstrated a novel QD based multi-section design where a passively mode-locked monolithic CPM laser is stabilized by injection of optical pulses from a stable high-Q passively mode-locked ring laser at a sub-harmonic of the cavity resonance frequency in an all-passive stabilization architecture [8]. Four-wave mixing (FWM) in the common SA is believed to be the primary mechanism for the locking which stabilizes and hence reduces the timing jitter as well as the long-term frequency drift of the CPM slave laser. A stable 30 GHz optical pulse train is generated and both the RF and optical linewidths are significantly reduced confirming the effectiveness of the FWM technique. In this letter, we describe an experiment to confirm FWM process to be responsible for the injection locking in our design. This is the first time, to the best of our knowledge that four-wave mixing has been conclusively shown to be used for injection locking in semiconductor media especially in an orthogonal waveguide configuration. It should be noted that the FWM has been suggested as a mechanism to couple two independent CPM dye ring lasers, however, no conclusive evidence was shown to support this assertion [9]. We also subsequently investigate the contributions from other mechanisms such as linear scattering, which are found to be negligible as expected in the case of low-index contrast perpendicular waveguide crossings [10], [11].

As seen in Fig. 1, the two curved gain sections are part of an external high-Q ring laser, which is precisely built and passively mode-locked at a sub-harmonic of the monolithic CPM laser. Under normal operating conditions, both lasers operate bidirectionally i.e., both lasers operate in the CPM regime. However, in order for the FWM effect to be unambiguously identified, a free space circulator is added to force unidirectional operation of the ring laser and allow access to the ASE output in backwards direction from the other facet (port-2) of the ring laser. When the two pulses from the crossed cavities overlap in the common SA region, they cause a carrier density variation leading to the formation of transient gratings at 45° to the face of the SA [12]–[14]. The 45° grating causes the third pulse to diffract into the orthogonal cavity, essentially locking the CPM laser to the ring laser. The pulse synchronization happens for the same reason that two counter-propagating pulses meet in the absorber of a conventional CPM laser. The counter-clockwise ASE output from port-2 of the ring laser is then analyzed before and after injection to confirm the FWM process. The emission is found to contain CPM light only in the presence of injection locking,

Manuscript received January 22, 2013; revised June 4, 2013; accepted June 17, 2013. Date of publication June 26, 2013; date of current version July 22, 2013. This work was supported by the Army Research Office under Contract W911NF-10-1-0189.

The authors are with CREOL, The College of Optics and Photonics, University of Central Florida, Orlando, FL 32816 USA (e-mail: aardey@creol.ucf.edu; esarailo@creol.ucf.edu; delfyett@creol.ucf.edu).

Color versions of one or more of the figures in this letter are available online at http://ieeexplore.ieee.org.

Digital Object Identifier 10.1109/LPT.2013.2271253

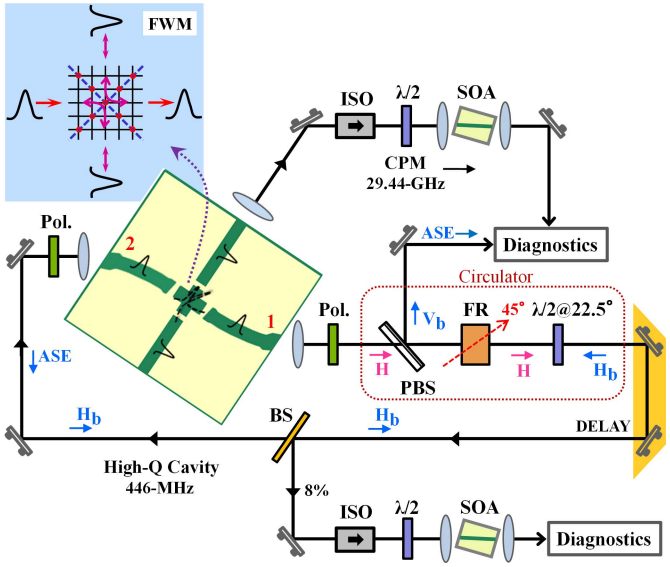

Fig. 1. A schematic of the experimental setup. The horizontal and vertical polarized light is shown using symbols H and V, respectively. The symbols H_b and V_b denote the polarization of the backward emitted ASE light in the counter-clockwise direction. The output ports of the external ring laser are marked as 1 and 2, respectively. ASE: amplified spontaneous emission. SOA: semiconductor optical amplifier. Pol: linear polarizer. PBS: polarizing beam splitter. FR: faraday rotator. BS: pellicle beam splitter. $\lambda/2$: half-wave plate. ISO: optical isolator.

which proves the FWM effect. Other linear scattering effects are proven to be non-existent by looking at the same ASE output from port-2 with and without the CPM laser lasing.

II. Device Design and Fabrication

The devices used in the experiment are the same as described in [8]. They are fabricated from InAs/InGaAs QD wafer grown by molecular beam epitaxy on a (001) oriented n+ GaAs substrate. The active region is a multi-stack QD structure, consisting of 10 layers of self-assembled InAs QDs capped by $In_XGa_{1-x}As$ QWs and bounded by AlGaAs cladding layers. Each QD layer is separated by 33 nm thick GaAs spacers. The devices emit at the telecom wavelength of $\sim$1.3 μm.

The fabricated monolithic device structure is shown in Fig. 2. It consists of four gain sections with two crossed SA's at the symmetry center of the cavity in order to maximize the coherent coupling of the four colliding pulses. Mesa structures are defined using standard ridge waveguide laser processing. The sample is wet-etched to form 3.6 and 4.6 μm wide single mode waveguides in the case of curved and linear sections, respectively. The curved section waveguides are designed at an angle of 7° with respect to the facet and are tapered to 4.6 μm widths at the termination to avoid Fabry-Perot (FP) reflections. The SA sections are 4.6 μm wide and 200 μm long waveguides, separated by a 15 μm gap from the gain sections. All the gain and SA sections are further angled relative to each other to avoid FP reflections. Benzocyclobutene (BCB) polymer is used for planarization and standard Ti-Au and Ni-Ge-Au metal contacts are used for the p- and n-side of the wafer after lapping and polishing. The gain sections are electrically isolated from each other, allowing for individual

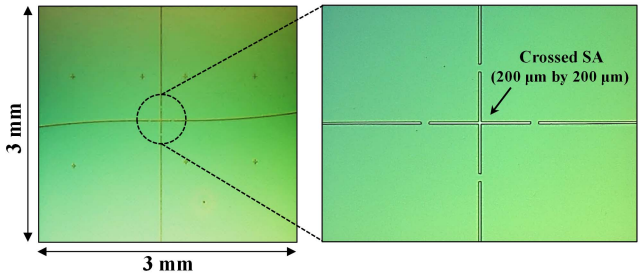

Fig. 2. (Left): Fabricated device before metallization with BCB as the isolation layer (seen in green). (Right): Magnified picture showing crossed saturable absorbers, each being 200 μm in length.

control of the DC bias currents to help achieve optimal mode-locking. No coating is applied to the cleaved facets. Single mode operation is verified using effective index method and beam profiling.

The semiconductor optical amplifiers (SOA) used to amplify the output of the lasers are fabricated using the same QD wafer and consist of 4 μm wide and 3 mm long ridge waveguide angled at 7° to the facet. The nominal small signal gain of these devices is around 21 dB. The multi-section device and the SOA's are mounted p-side up on a copper heat sink and are maintained at a constant temperature (20 °C) using a thermoelectric cooler.

III. Experimental Setup

Fig. 1 illustrates the experimental schematic. The monolithic CPM cavity is cleaved at a length of 2.8 mm and is passively mode-locked by applying a negative bias voltage to the SA section. With a forward bias current of $\sim$25 mA on each of the linear gain section and a reverse bias voltage of -6.1 V $\pm$ 0.1 V on the SA, the laser typically emits close to transform limited pulses of some few picoseconds. It should be noted that because of two counter-propagating pulses traveling simultaneously in the cavity, the repetition rate in the CPM configuration is twice the free spectral range (FSR) of the whole cavity. The monolithic CPM cavity thus has a pulse repetition rate of $\sim$29.44 GHz.

The external high-Q ring laser is built using four gold coated external mirrors, with two mirrors mounted on a translation stage to control and precisely match the cavity length to a sub-harmonic of the CPM laser. The chosen cavity length corresponds to an FSR of 446 MHz, which is the 66^{th} sub-harmonic of the CPM laser. A free space optical circulator is build inside the cavity with the help of a polarizing beam splitter (PBS), faraday rotator (FR) and a half-wave plate. This allows the cavity to operate unidirectional (clockwise) while simultaneously giving access to the ASE output emitted from the other facet in the counter-clockwise direction. Because of the non-reciprocity of the FR, this ASE component is vertically polarized and thus coupled out using the same PBS for analysis. Note that the light emitted from the semiconductor diode laser is horizontally polarized (TE) to begin with and care is taken to maintain that polarization by placing linear polarizer's at the outputs of the laser, which eliminates any residual vertical polarized light component arising from the

minute tilt of the device while mounting. Passive mode-locking is achieved by applying a reverse bias voltage of −6.1 V on the common SA region, which is shared and kept constant with the SA of the CPM laser. The corresponding forward bias current used is 80 mA on each of the curved gain sections giving a pulsewidth of around 5 ps. The mode-locked optical and RF spectra are shown in Fig. 3(a) and (b).

The reverse bias voltage and bias currents used in the experiment are carefully chosen to achieve simultaneous stable mode-locking of the external cavity laser and the CPM laser and to achieve optical spectral overlap of the two cavities. The spectral overlap induces coupling between the two cavities whereby the injected pulses transfer the phase stability to the longitudinal modes of the CPM slave laser, thus injection locking the CPM laser to the master external cavity.

IV. Measurement and Results

Injection locking is first verified by examining the RF and optical spectra of the CPM laser for reduction in the RF linewidth and for optical supermode suppression, shown in Fig. 3(c) and (d). As seen, the reduction is not as drastic as observed in the earlier work [8], because of the three-pulse interaction in the current setup as opposed to four pulses, though it's sufficient to achieve FWM and injection lock the CPM laser. The measurements before injection are taken by physically blocking the light inside the master ring cavity. Optical pulse injection is achieved by removing this beam block. Fig. 4(a) shows the optical spectrum of the backward propagating ASE output from port-2 of the external ring laser before and after injection. As seen in the figure, because of the back reflections from the circulator optics inside the external ring cavity, we do get leakage of the ring cavity lasing spectrum coupled to the ASE output, which though small can affect our measurements. The presence of the CPM light is then highlighted by examining the background subtracted ASE before and after injection locking. This is obtained by subtracting the two measured spectra shown in Fig. 4(a) displaying the result in Fig. 4(b). In the resultant difference spectra, the center of the spectrum clearly shows the diffracted spectra of the CPM laser which matches the location where the CPM mode-locked peak otherwise would fall. It should be noted that the normal output of the 29.44 GHz CPM laser shows an axial mode spacing of 29.44 GHz. This is because there are two coherent pulse trains oscillating in a 14.72 GHz cavity, but temporally delayed by half-round trip. The resulting output thus displays an axial mode spacing of 29.44 GHz due to the spectral interference and resulting spectral modulation caused by the temporal delay of the two-pulse trains of ∼34 ps. On the other hand, the output spectrum of the FWM signal shows an axial mode spacing of 14.72 GHz. This is because the two coherent pulse trains that possess axial modes at 14.72 GHz are diffracted simultaneously i.e., both pulse trains are temporally overlapped in time, resulting in observed spectra with axial modes at 14.72 GHz. Finally, it should be noted that the diffracted pulse occurs only every ∼2 ns. This produces an additional spectral substructure at 446 MHz which is not spectrally resolved.

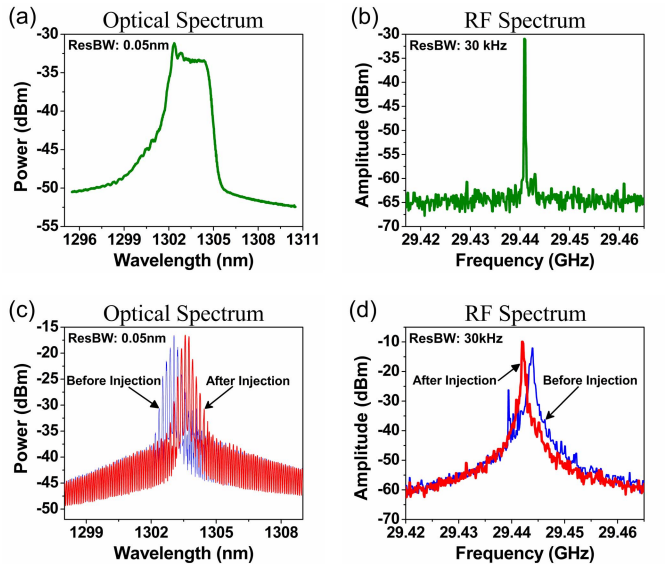

Fig. 3. (a), (b): Typical spectra of the passively mode-locked high-Q external cavity (master) laser. (c), (d): Typical spectra of the passively mode-locked CPM (slave) laser before (in blue) and after (in red) optical injection.

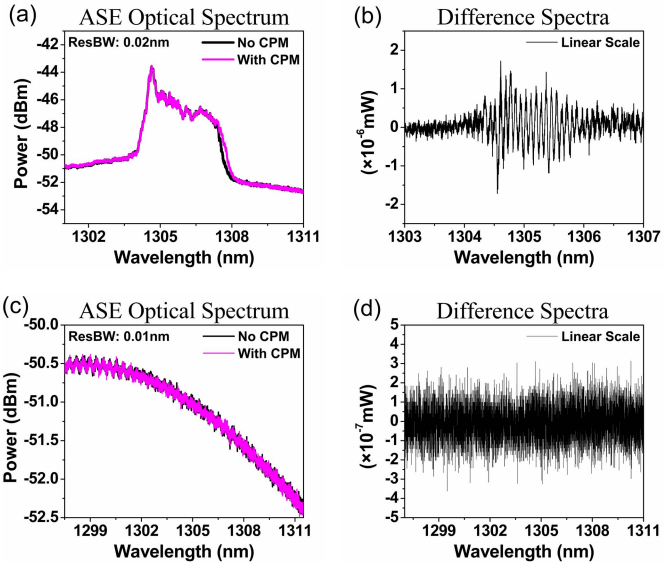

Fig. 4. (a): Backward propagating ASE spectra from port-2 of the passively mode-locked high-Q external cavity (master) laser with and without injection of the CPM laser. Also seen is the back reflected leakage light from the intra-cavity optics superimposed on the ASE spectra. (b): Background subtracted spectra from Fig. 4(a), showing the diffracted CPM spectra present in port-2 due to FWM. (c): ASE spectra from port-2 of the master laser with port-1 physically blocked. (d): Background subtracted spectra from Fig. 4(c), with no residual CPM laser light observed in the absence of FWM.

To make sure that the observed CPM light superimposed on top of the ASE output is only due to the aforementioned FWM and not due to any other linear scattering effect, we also measure the same ASE output from the ring cavity laser with and without CPM lasing while physically blocking port-1 before the PBS and keeping all the bias conditions the same. Any leakage of the CPM light into the ring cavity would then be seen in the measured optical spectrum. However, as seen in Fig. 4(d), the resultant subtracted spectrum with and without the port-1 blocked shows no residual CPM light, confirming

that FWM is the primary mechanism for the injection locking in our design.

V. Conclusion

To summarize, we have experimentally confirmed that FWM is indeed the primary mechanism responsible for the interaction and locking of the CPM laser. This stabilizes and thus effectively reduces the jitter associated with the CPM laser as shown in our earlier work [8]. Other linear scattering effects, which are predicted to be small as in [10], [11] are also investigated and found be negligible. These results confirm the potential of the new and simple optical injection locking technique as the stabilization technique that can be used in the future large scale designing of monolithically integrated devices with the benefit of a standard fabrication process and the cost-effectiveness of semiconductor material. Also with the novel techniques recently demonstrated, such as active-passive waveguide integration and long low-loss passive waveguides (in III-V/Silicon), in the near future the narrow linewidth CPM laser employing the new FWM technique can be fabricated with the high-Q cavity in an all-monolithic architecture. With a stabilized pulse train, this ultra-compact and ultrashort optical source would be attractive for use in the forthcoming photonic access networks employing technologies such as dense wavelength-division multiplexing (DWDM) and ultra-high speed OTDM.

References

[1] S. Arahira, and Y. Ogawa, "480-GHz sub-harmonic synchronous mode-locking in a short-cavity colliding-pulse mode-locked laser diode," *IEEE Photon. Technol. Lett.*, vol. 14, no. 4, pp. 537–539, Apr. 2002.

[2] Y. K. Chen and M. C. Wu, "Monolithic colliding-pulse mode-locked quantum-well lasers," *IEEE J. Quantum Electron.*, vol. 28, no. 10, pp. 2176–2185, Oct. 1992.

[3] E. U. Rafailov, M. A. Cataluna, and W. Sibbett, "Mode-locked quantum-dot lasers," *Nat. Photon.*, vol. 1, pp. 395–401, Jul. 2007.

[4] M. G. Thompson, A. R. Rae, M. Xia, R. V. Penty, and I. H. White, "InGaAs quantum-dot mode-locked laser diodes," *IEEE J. Sel. Topic Quantum Electron.*, vol. 15, no. 3, pp. 661–672, May/Jun. 2009.

[5] X. Huang, A. Stintz, H. Li, L. F. Lester, J. Cheng, and K. J. Malloy, "Passive mode-locking in 1.3 μm two-section InAs quantum dot lasers," *Appl. Phys. Lett.*, vol. 78, no. 19, pp. 2825–2826, May 2001.

[6] G. Carpintero, M. G. Thompson, K. Yvind, R. V. Penty, and I. H. White, "Comparison of the noise performance of 10 GHz repetition rate quantum-dot and quantum well monolithic mode-locked semiconductor lasers," *IET Optoelectron.*, vol. 5, no. 5, pp. 195–201, Oct. 2011.

[7] D. J. Derickson, P. A. Morton, J. E. Bowers, and R. L. Thornton, "Comparison of timing jitter in external and monolithic cavity mode-locked semiconductor lasers," *Appl. Phys. Lett.*, vol. 59, no. 26, pp. 3372–3374, Dec. 1991.

[8] A. Ardey, J. Kim, E. Sarailou, and P. J. Delfyett, "Optical and RF stability transfer in a monolithic coupled-cavity colliding pulse mode-locked quantum dot laser," *Opt. Lett.*, vol. 37, no. 17, pp. 3480–3482, Sep. 2012.

[9] S. Wu, S. L. Smith, and R. L. Fork, "Kerr-lens-mediated dynamics of two nonlinearly coupled mode-locked laser oscillators," *Opt. Lett.*, vol. 17, no. 4, pp. 276–278, Sep. 2012.

[10] M. G. Daly, P. E. Jessop, and D. Yevick, "Crosstalk reduction in intersecting rib waveguides," *J. Lightw. Technol.*, vol. 14, no. 7, pp. 1695–1698, Jul. 1996.

[11] C. van Dam, F. P. G. M. van Ham, F. H. Groen, J. J. G. M. van der Tol, I. Moerman, and M. K. Smit, "Compact InP-based waveguide crossings with low crosstalk and low loss," in *Proc. Conf. Integr. Photon. Res.*, vol. 6. Apr. 1996, pp. 1–5, paper IMH-1.

[12] D. Kühlke, W. Rudolph, and B. Wilhelmi, "Influence of transient absorber gratings on the pulse parameters of passively mode-locked CW dye ring lasers," *Appl. Phys. Lett.*, vol. 42, no. 4, pp. 325–327, Feb. 1983.

[13] J. Buchert, R. Dorsinville, P. Delfyett, S. Krimchansky, and R. R. Alfano, "Determination of temporal correlation of ultrafast laser pulses using phase conjugation," *Opt. Commun.*, vol. 52, no. 6, pp. 433–437, Jan. 1985.

[14] P. P. Vasil'ev, V. N. Morzov, Y. M. Popov, and A. B. Sergeev, "Subpicosecond pulse generation by a tandem-type AlGaAs DH laser with colliding pulse mode locking," *IEEE J. Quantum Electron.*, vol. 22, no. 1, pp. 149–152, Jan. 1986.